Article

Assessment of the Permeability to Aggressive Agents of Concrete with Recycled Cement and Mixed Recycled Aggregate

Blas Cantero [1], Miguel Bravo [2], Jorge de Brito [3,*], Isabel Fuencisla Sáez del Bosque [1] and César Medina [1]

[1] UEX-CSIC Partnering Unit, Department of Construction, Institute for Sustainable Regional Development (INTERRA), School of Engineering, University of Extremadura, 1003 Cáceres, Spain; bcanteroch@unex.es (B.C.); isaezdelu@unex.es (I.F.S.d.B.); cmedinam@unex.es (C.M.)

[2] CERIS, Department of Civil Engineering, Barreiro School of Technology, Polytechnic Institute of Setúbal, Rua Américo da Silva Marinho, 2839-001 Lavradio, Portugal; miguelnbravo@tecnico.ulisboa.pt

[3] CERIS, Department of Civil Engineering, Architecture and Georresources, Instituto Superior Técnico (IST), Universidade de Lisboa, 10071 Lisbon, Portugal

* Correspondence: jb@civil.ist.utl.pt; Tel.: +351-218-419-709; Fax: +351-218-497-650

Abstract: Acceptance by the construction industry of recycled concrete as a sustainable alternative material is contingent upon a reliable assessment of its permeability to corrosive agents. This study analyses the transport mechanisms associated with chloride (Cl^-), oxygen (O_2) and carbon dioxide (CO_2) ions in concrete with cement made with 10% or 25% ground recycled concrete (GRC) separately or in combination with 50% mixed recycled aggregate (MRA). The findings show that, irrespective of aggregate type, concrete with GRC exhibited lower resistance to ingress than conventional concrete due to its greater porosity. Nonetheless, O_2 permeability was consistently below 4.5×10^{-17} m^2 and CO_2 penetration, under 4 mm/$year^{0.5}$, indicative of concrete with high quality. Resistance to CO_2 and Cl^- penetration in the materials with 10% GRC was similar to the values observed in conventional concrete. On the other hand, the incorporation of 25% GRC increased the penetration of CO_2 and Cl^- by 106% and 38%, respectively. Further to those findings in normal carbonation environments, reinforcement passivity would be guaranteed in such recycled materials over a 100 year service life.

Keywords: recycled aggregate; recycled concrete; durability; chloride penetration; carbonation

1. Introduction

The evaluation of the mechanical behaviour of concrete is always considered essential, while the evaluation of the durability of this construction material is sometimes overlooked. Concrete with high porosity allows the entry of external agents, which can lead to durability problems; hence, it is essential to study in detail several properties that are related to the durability of concrete.

The permeability to aggressive agents in concrete can be measured through several tests, such as evaluating the transport mechanisms associated with chloride ions, oxygen and carbon dioxide.

The analysis of the permeability of concrete to gases concerns the entire porous structure of this material, i.e., both small and large pores, due to the reduced size of the oxygen molecules. Therefore, the oxygen permeability test has a higher sensitivity than the water absorption tests, since the water molecules are larger than the oxygen ones [1].

The transport mechanism of chloride ions in concrete is somewhat complex, and may involve diffusion, impregnation and capillary water absorption processes. Transport mechanisms vary widely with the microenvironment in which the structural elements are inserted. The penetration of chlorides into ordinary concrete is usually carried out through the continuous pore structure of the cementitious paste, the interface between the aggregates, and the paste (ITZ) and micro-cracks [2]. The penetration of chlorides is, together with carbonation, the main factor responsible for the depassivation and corrosion of steel reinforcement in reinforced concrete.

In turn, the carbonation process begins with the penetration, by diffusion, of carbon dioxide (CO_2) into concrete, which, in the presence of moisture, reacts with the hydrated cement minerals and gives rise to carbonation. In other words, CO_2 in the atmosphere reacts with the alkaline components of concrete, namely by transforming calcium hydroxide (CH) into calcium carbonate. These chemical reactions of dissolution of the crystalline phases of concrete cause a decrease in the pH of the concrete pores' solution, enabling the corrosion of the steel reinforcement, since the oxide film that protects the steel reinforcement is only stable in very alkaline environments [3]. The carbonation resistance of concrete is generally determined through accelerated tests, in which the concrete specimens are subjected to high concentrations of CO_2 (5%). Thus, one of the problems of this type of test is to understand whether the results obtained evaluate rigorously the behaviour of concrete exposed to atmospheric CO_2 concentrations. It is recalled that the concentration, in volume, of CO_2 in the atmosphere usually varies between 0.03%, in rural areas, and 0.10%, in places with high population density [4].

According to data presented by the United Nations, in 2015 the world population was around 7.3 billion, and this number is expected to reach 9.7 billion in 2050 [5]. That report also indicates that, in 2015, for the first time, the majority of the world's population already lived in cities. The migration of populations to urbanized areas brings benefits for global development, but also implies a significant increase in built parks, with an increase in the production of construction and demolition waste (CDW), whose environmental impact is extremely negative. Although the use of CDW already occurs, as aggregates in concrete in some constructions, the truth is that its incorporation still corresponds to occasional cases and it is not a common reality.

The use of recycled aggregates (RA) in concrete raises some important questions in terms of durability. These aggregates have physical properties and compositions that are very different from those of natural aggregates. The main difference is related to the greater porosity and, consequently, greater water absorption of RA. However, this variation depends on the RA's source and production process. On the other hand, the roughness and specific surface of RA are usually higher and RA typically have more elongated shapes. Due to these factors, the effective water/cement (w/c) ratio of mixes with RA must be increased to maintain a given workability, which then leads to more porous cementitious matrices and interfacial transition zones (ITZs). Given this, the use of RA in concrete can decrease its durability [6].

On the other hand, in the 20th century, the annual emission of carbon dioxide (CO_2) into the atmosphere increased from 1.5 to 25 billion tonnes [7]. This unsustainable rate of emissions comes from several activities, including construction, which alone contributes to more than 6% of the global value through the production of cement. Thus, it is important to investigate the possibility of providing the construction industry with an innovative way of creating structural concrete with a positive environmental impact throughout its life cycle. This can be achieved through the creation of synergies in two distinct areas: replacement of the Portland cement by an alternative binder with lower environmental impact using CDW; and incorporation of RA from CDW.

According to this literature review, there are not many studies on the behaviour in terms of durability of concrete with CDW simultaneously used as aggregates and binders. The use of CDW in concrete has been analysed mainly in two different ways: analysis of the use of RA from crushed concrete; and evaluation of the use of RA from mixed CDW. The latter RA have highly variable composition, which makes their analysis more difficult. On the other hand, RA from CDW generally have higher water absorption, which causes some limitations on their use in concrete.

Torgal et al. [8] analysed the oxygen permeability of concrete with RA and recycled cement from four types of ceramics (ceramic bricks, double-fired white stoneware, sanitary ware and single-fired white stoneware). The authors found that the replacement of 20% Portland cement with recycled cement from ceramics leads to maintaining the oxygen permeability of concrete. For two of the wastes (double-fired and single-fired white

stoneware), there was even a slight improvement in this property (lower than 10%). In turn, the authors observed an improvement of 20% and 30% in oxygen permeability with the total replacement of coarse and fine aggregates, respectively. The authors explain this result with the highest degree of hydration in the cementitious paste of concrete with RA.

Thomas et al. [9] evaluated some properties of precast concrete elements in which coarse RA and recycled cement were used. In this experimental campaign, six concrete mixes were characterised: a reference mix; two mixes with 25% and 50% (by weight) RA from mixed CDW; three mixes similar to the previous ones but with recycled cement with low clinker content (cement produced with 25% of ceramic waste). As in other studies [6], it was found that the oxygen permeability coefficient increases with the replacement of natural aggregates with RA. The authors [9] also concluded that this increase is higher in concrete with recycled cement and with the use of 50% of RA (higher than 300%) than in concrete with Portland cement and with the use of 50% of RA (higher than 40%).

Bravo et al. [6] studied the replacement of natural aggregates (fine and coarse) by RA from mixed CDW from four recycling plants. To this end, the authors analysed the oxygen permeability of concrete produced with 0%, 10%, 50% and 100% of fine or coarse RA. Total replacement of the fine and coarse aggregates caused increases in this property of more than 43% and 91%, respectively. Thomas et al. [9] also obtained significant increases in this property with the incorporation of coarse RA from CDW. The authors obtained increases of 50% in the oxygen permeability test performed at 28 days.

Torgal et al. [8] also evaluated the resistance to the penetration of chloride ions in concrete with RA (ceramic) and recycled cement (from four types of ceramic waste). The authors concluded that the use of RA and recycled cement significantly improved this property, obtaining decreases in the diffusion of chloride ions between 12% and 70%, and between 23% and 29%, respectively.

Qin and Gao [10] analysed the influence of the use of recycled cement produced from concrete waste (0%, 10%, 20%, 30% and 50% of the total weight of the binders) on the resistance to the penetration of chloride ions of cementitious composites. The authors concluded that the use of 50% recycled cement increases the permeability to chloride ions by more than 300%. However, the authors found that this increase is reduced to around 200% when the concrete is subjected to accelerated carbonation curing.

Some studies have also analysed the carbonation resistance of concrete with recycled cement. Kim [11] evaluated the behaviour of self-consolidating concrete with recycled cement from concrete (0%, 15%, 30% and 45% of the total mass of the binders). The author found that the use of this recycled cement causes a significant increase in the carbonation depth of the concrete (between 2.3 and 6.9 times).

Sáez del Bosque et al. [12] also evaluated the carbonation resistance of concrete with coarse RA from CDW (25% and 50% of the total coarse aggregates) and recycled cement (with 25% of ceramic wastes). Regardless of the type of cement, the average carbonation depth was slightly higher in materials with 25% or 50% recycled aggregate than in the reference concrete. The use of this partially recycled cement produced from ceramic waste led to an increase in the carbonation depth at 28 days from 4.2 mm to 5.0 mm (increase of 19%).

The present investigation follows previous ones that intended to analyse the mechanical behaviour, water absorption, shrinkage and thermal performance of concrete with RA from CDW and recycled cement [13–15]. In these previous investigations, the authors observed that the use of GRC enhanced concrete environmental performance. At 10% replacement, it lowered the CO_2 emitted in concrete manufacture by 7.5%, and at 25% GRC by 18.7%, relative to concrete made with ordinary Portland cement (OPC).

There are already some studies that address the permeability of concrete with recycled cement (mainly from ceramic wastes) or with RA from CDW. However, no previous study has evaluated the permeability to aggressive agents (chloride ions, carbon dioxide and oxygen) of concrete with simultaneous replacement of the two elements evaluated in this investigation. To fill this scientific and technical knowledge gap, this study analyses the

effect of replacing Portland cement with ground recycled cement (GRC), at 10% (R10) or 25% (R25). This assessment was carried out on concrete with 100% NA, 50% NA and 50% mixed recycled aggregates (MRA). This experimental campaign involved the evaluation of the permeability to the aggressive agents of these mixes through the performance of oxygen permeability tests, resistance to the penetration of chloride ions and resistance to carbonation. Finally, the evolution of the carbonation front in these mixes was studied with the increase in the exposure time for mixes in different exposure classes, according to the forecasting model proposed by EHE-08 [16]. This assessment in this type of concrete has not yet been carried out in previous investigations.

2. Experimental Programme

2.1. Materials

2.1.1. Binders

The three types of binders used in this study were as follows: (i) type I 42.5 R (CEM I 42.5 R) ordinary Portland cement (OPC); (ii) a binder with 90% OPC and 10% GRC; and (iii) a binder with 75% OPC and 25% GRC. The GRC was obtained by crushing and grinding laboratory-prepared concrete specimens (stored in a wet chamber at $20 \pm 2\,^{\circ}\text{C}$ and relative humidity of $55 \pm 5\%$ for 90 days), batched as per the Faury method with $300\,\text{kg/m}^3$ of cement and a water/binder ratio of 0.55. The GRC processing is illustrated in Figure 1: (i) in Stage 1, the specimens were mixed, moulded, cured and subsequently tested to breakage; (ii) in Stage 2, the cubic and prismatic specimens were jaw-crushed to a particle size of <16 mm; (iii) in Stage 3, the particles generated in Stage 2 were roll-crushed to <5 mm; and (iv) in Stage 4, the crushed concrete was ball-ground for 2 h at 60 rpm (ratio between abrasive load and material of 3/1) to the target fineness.
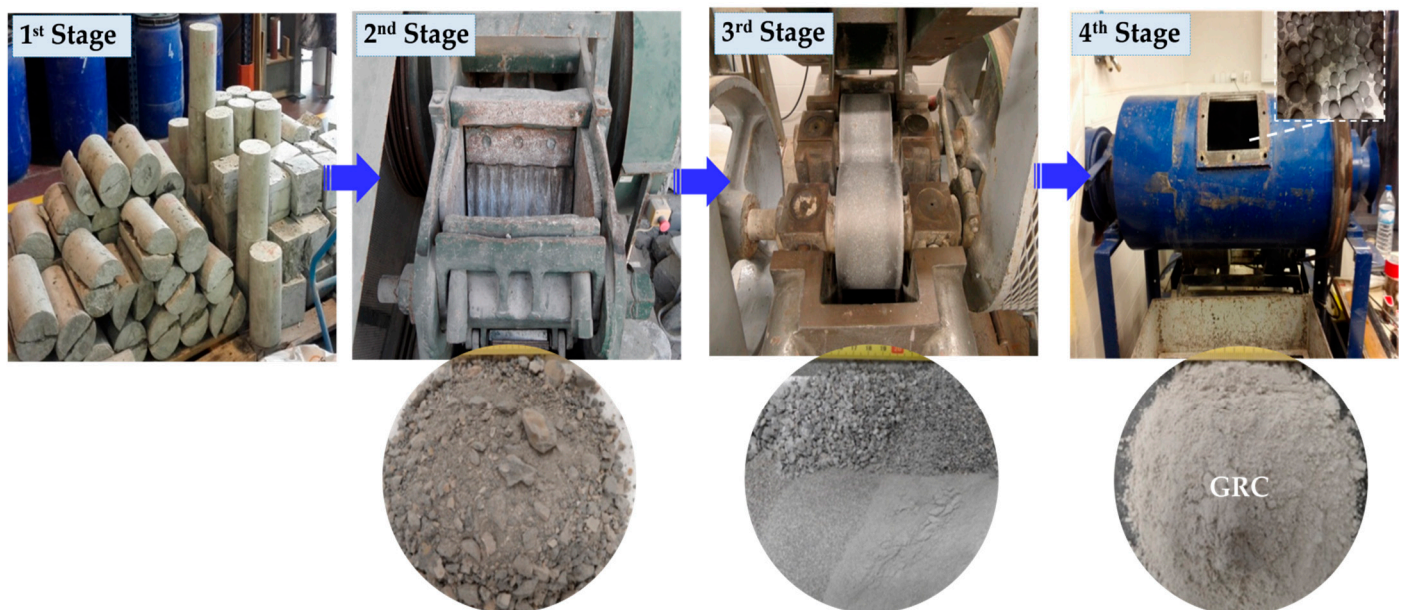
Figure 1. Four stages of GRC preparation.

OPC's and GRC's chemical compositions, particle size distributions and densities are given in Table 1. The main phases in GRC are SiO_2 (46.1 wt%); CaO (40.0 wt%); and Al_2O_3 (5.3 wt%).

D_{90} (90th percentile value for particle diameter) in GRC was 147 μm. The difference from the 46 μm recorded for OPC is associated with the natural aggregate present in the source recycled concrete. In contrast, the lower value of D_{10} in the GRC (1.58 μm) than for OPC may be attributed to the presence of a cementitious matrix in the recycled

aggregate used to prepare the former. The GRC used was less dense (2.54 g/cm^3) than OPC (3.11 g/cm^3).

Table 1. Chemical constituents and physical properties of OPC and GRC.

Material	Chemical Constituent (wt%)								
	SiO$_2$	CaO	Al$_2$O$_3$	Fe$_2$O$_3$	Na$_2$O	K$_2$O	MgO	SO$_3$	LoI *
OPC	18.7	65.1	5.1	2.6	0.2	0.5	1.8	3.0	2.5
GRC	46.1	40.0	3.8	1.5	0.3	1.2	0.5	0.4	6.2
	Physical Property								
	Sieve size (μm)			Per cent passing (%)		Density (g/cm^3)			
	10	50	90	<63 μm					
OPC	1.9	13.8	46.0	97.9		3.1			
GRC	1.6	21.2	147.0	67.8		2.5			

Note. * LoI: loss on ignition.

2.1.2. Aggregates

The coarse natural aggregate (NA) used contained two sizes of limestone gravel, 4/12 mm (NG-M) and 12/22 mm (NG-G), and two sizes of siliceous river sand, 0/2 mm (NS-F) and 2/4 mm (NS-C). The single fraction (0/32 mm) MRA supplied by a CDW recycling plant at Lisbon (Portugal) was sieved and classified at the laboratory, where sizes <4 mm and >22 mm were discarded. The particle size distributions of all the NA and of the 4/22 mm coarse MRA aggregate ultimately used complied with the recommendations of European standard EN 933-1 [17] and are given in Figure 2.
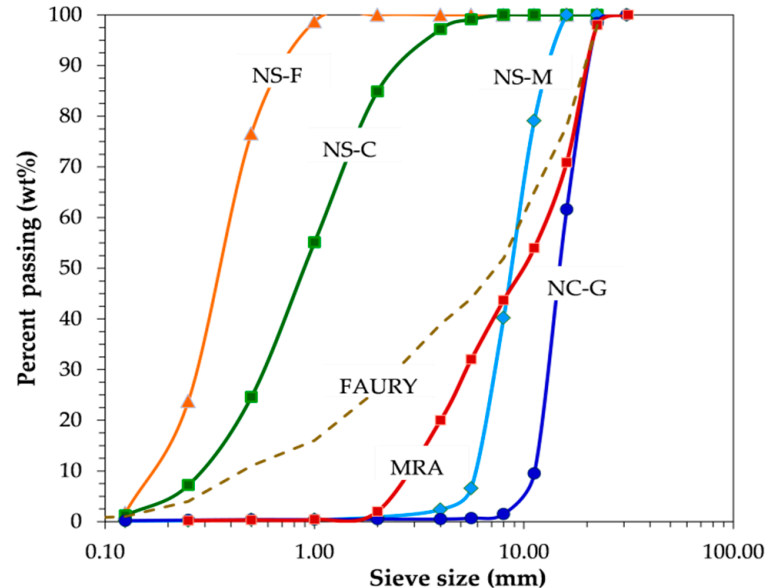

Figure 2. Aggregate particle size distribution and theoretical Faury curve for a maximum aggregate size of 22 mm and 300 kg/cm^3 cement.

The composition of the 4/22 mm coarse MRA aggregate, likewise determined as per standard EN 933-11 [18], is listed in Table 2, according to which the main components were Rc (47.1 wt%), Rb (22.3 wt%) and Ru (25.2 wt%), with glass and plaster (<2 wt%) as minor constituents. On the grounds of those data and the criteria set out in Spain's structural concrete code (EHE-08) [16], with its <95 wt% Rcu (Rcu = Rc + Ru) content and >5 wt% Rb content, MRA qualified for classification as a mixed recycled aggregate. The physical and mechanical properties recommended in standard EN 12620 [19] for coarse aggregates to be used in structural concrete (f$_{ck}$ ≤ 30 MPa) are listed in Table 3.

Table 2. Composition of MRA as per standard EN 12620.

Class	Rc	Ru	Rb	Rg	Ra	X1	X2	FL
Amount (wt%)	47.1	25.2	22.6	1.7	0.2	1.8	0.4	1.0

Component abbreviations: Rc: concrete and mortar, Ru: natural stone, Rb: clay materials, Rg: glass, Ra: bituminous matter, X1: gypsum, X2: metals, FL: floating particles.

Table 3. Physical and mechanical properties of the aggregates.

Property	NS-F	NS-C	NC-M	NC-G	MRA	EN 12620
Dry density (kg/m^3) [20]	2581	2583	2600	2620	2069	-
SSD [1] density (kg/m^3) [20]	2601	2609	2630	2670	2256	-
$WA_{24 h}$ [2] (wt%) [20]	0.4	0.5	1.3	1.3	9.1	≤ 5 (≤ 7) [5]
$WA_{10 min}$ (wt%) [21]	0.2	0.3	0.5	0.6	8.1	-
Open porosity (vol%) [20]	1.1	1.2	2.5	3	18.7	-
LA [3] (wt%) [22]	-	-	28	26	46	≤ 40 [6]
FI [4] (wt%) [23]	-	-	13	16	20	<35

Aggregate abbreviations: NS-F: natural fine sand (0/2 mm); NS-C: natural coarse sand (2/4 mm); NC-M: natural medium gravel (4/12 mm); NC-G: natural coarse gravel (12/22 mm); MRA: mixed recycled aggregate (4/22 mm). **Note.** [1] SSD: saturated surface dry, [2] WA: water absorption, [3] LA: Los Angeles coefficient, [4] FI: flakiness index, [5] concrete with compressive strength < 30 MPa; and [6] blended recycled and natural aggregate according to Spanish concrete code EHE-08 [16].

2.2. Experimental Procedure

2.2.1. Pre-Conditioning

The specimens were prepared and cured for the O_2 permeability and CO_2 and Cl^- penetration tests as per European standard EN 12390-2 [24]. The size of the prismatic specimens for O_2 permeability testing was 150 × 300 mm ($\varnothing$ × height) and that of the samples for CO_2 and Cl$^-$ penetration was 100 × 200 mm. All of the specimens were cured for 28 d or 90 d in a wet chamber at a relative humidity of 95 ± 5% and a temperature of 20 ± 2 °C. Concrete disks 50 mm thick (measured with a digital calliper with a precision of 0.1 mm) were cut out of the mid-section of each specimen with a water-cooled diamond saw. The samples for O_2 permeability and Cl$^-$ penetration testing were subsequently sealed around the outer rims and the disks for the CO_2 penetration tests at the top and bottom with three layers of epoxy resin to ensure one-dimensional flow.

The samples for the O_2 permeability and CO_2 penetration tests were stored in a wet chamber at 20 ± 2 °C and relative humidity of 55 ± 5% for 3 weeks, in keeping with standardised procedures. The samples for the Cl^- penetration tests were pre-saturated for 4 h in a vacuum container with the top and bottom exposed to the ultra-low pressure (<1 mm Hg). Water was then added to the container, where the vacuum was released after 1 h and the samples left to soak in the water for a further 18 ± 2 h prior to testing.

2.2.2. Oxygen Permeability

O_2 permeability was assessed with a Cembureau apparatus in a room at the controlled temperature (20 ± 2 °C) and relative humidity (50 ± 5%) as specified in Spanish standard UNE 83981 [25]. The O_2 permeability coefficient, defined in terms of Darcy's law, was calculated here with the Hagen–Poiseuille relationship (Equation (1)) for the laminar flow of a compressible fluid across a porous medium under steady flow conditions [26]:

$$K = \frac{2\mu L}{S\left(P_s^2 - P_O^2\right)} P_s Q_s \tag{1}$$

where K (m^2) is the O_2 permeability coefficient; Q_s the outlet flow ($m^3 \cdot s^{-1}$); P_s, the absolute pressure at the sample outlet (Nm^{-2}); P_o, the absolute pressure at the sample inlet (Nm^{-2});

S, the cross-sectional area of the sample (m^2); *L*, the sample thickness in the direction of the flow (m); and μ, the O_2 dynamic viscosity at 20 °C (2.02 × 10^{-5} Nsm^{-2}).

2.2.3. Rapid Chloride Permeability (RCP) Test

Cl$^-$ penetration was determined using the electrical procedure described in standard ASTM 1202-97 [27] in a room at a controlled temperature (20 ± 5 °C). The total electric current passing through the samples in 6 h was calculated by integrating current over time (RCP test finding), as in Equation (2):

$$RCP = 900(I_0 + 2I_{30} + 2I_{60} + \cdots + 2I_{300} + 2I_{330} + I_{360}) \tag{2}$$

where *RCP* is total charge (coulombs); I_o, the electric current immediately after applying voltage (Ampere); and I_t, the electric current at time *t* (Ampere), with subscripts denoting time in minutes.

The empirical formula proposed by Berke and Hicks [28] (Equation (3)) was applied to correlate *RCP* to the diffusion coefficient (*D*) in m^2/s × 10^{-12}:

$$D = 0.0103 \times RCP^{0.84} \tag{3}$$

where the unit for *RCP* is Coulomb.

2.2.4. Accelerated Carbonation Test

The resistance to CO_2 penetration test was conducted as described in Portuguese standard LNEC E391 [29]. The samples were stored for 7 d, 28 d, 56 d or 90 d in an accelerated carbonation chamber with a CO_2 concentration of 3 ± 0.1%, relative humidity of 60 ± 5% and temperature of 23 ± 3 °C. The carbonation depth was found by spraying the two sides of the sample resulting from diametric breakage with a phenolphthalein solution (0.8 g of the indicator in powder form dissolved in a solution containing 70 mL of ethanol and 30 mL of deionised water). As phenolphthalein is purple at pH > 10, the colourless concrete was determined to have been carbonated (pH < 8). Measurements were taken at a total of 12 points in each sample and recorded along with the maximum and minimum CO_2 penetration depths.

2.2.5. Service Life Prediction

Concrete carbonation affects the durability limit states of concrete structures, insofar as it deteriorates the passive cover that protects the reinforcing steel [30]. In the semi-probabilistic approach adopted by Spain's structural concrete code EHE-08, the condition to be met is as follows:

$$t_s > t_d \tag{4}$$

where t_s is estimated service life and t_d service life calculated for the concrete structure.

Calculated service life (t_d) is defined (Equation (5)) as the product of the design service life (t_{SL}) for the type of structure times a service life safety coefficient (γ_i), quantified in the aforementioned code as 1.10. A 50 year design service life is assumed for residential or office buildings, bridges and flyovers less than 10 m long and low- or medium-order engineering structures, whereas monumental buildings or high-order structures are designed for a 100 year service life:

$$t_d = \gamma_i \times t_{SL} \tag{5}$$

Further to the CO_2 penetration model described in code EHE-08 [16], characteristic depth (X$_c$) can be expressed as in Equation (6):

$$X_c(t_{SL)} = K_n \sqrt{t_d} \tag{6}$$

where X_c is the characteristic depth (mm) for the design service life; K_n is the natural carbonation coefficient listed in Table 8 (mm/year$^{0.5}$) and t_d, the calculated service life.

2.3. Concrete Design

Batching for all the concrete mixes is given in Table 4. In all mixes, irrespective of the MRA and/or NA content, the particle size distribution was fitted to Faury's [31] theoretical curve for a maximum aggregate size of 22 mm, maximum compactness and the same volume of aggregate in all mixes. That called for separating the MRA into sub-fractions: 16/22 mm, 11.2/16 mm, 8/11.2 mm, 5.6/8 mm, 4/5.6 mm. All the mixes were designed to meet the requirements set out in European standard EN-206-1 [32] for durability class XC2 and strength class C25/30. Cement was added at a rate of 300 kg/m^3 and all the mixes were prepared to S2 workability, defined in European standard EN-206-01 [32] as equivalent to a slump of 70 ± 20 mm [33]. Consequently, a higher water/binder ratio was required in the recycled materials than in the conventional materials due to the lower density of the GRC than OPC, and MRA than NA [15,34].

Table 4. Concrete mixes' compositions.

Material	Proportion (% or kg/m^3)					
Concrete Mix	**NAC**	**N10/0**	**N25/0**	**R0/50**	**R10/50**	**R25/50**
MRA replacement		0%			50%	
GRC replacement	0%	10%	25%	0%	10%	25%
OPC	300	270	225	300	270	225
GRC	-	30	75	-	30	75
Total water	168	174	180	205	211	217
[w/b(OPC+GRC)]	0.56	0.58	0.60	0.59	0.61	0.63
NS-F	154	150	154	154	154	154
NS-C	755	755	755	755	755	755
NG-M	367	367	367	184	184	184
NG-G	653	653	653	327	327	327
MRA 16–22 mm	-	-	-	109	109	109
MRA 11.2–16 mm	-	-	-	182	182	182
MRA 8–11.2 mm	-	-	-	85	85	85
MRA 5.6–8 mm	-	-	-	59	59	59
MRA 4–5.6 mm	-	-	-	14	14	14
Fresh and hardened concrete properties ($\pm$: standard deviation).						
Slump (mm)	65 ± 2.8	74 ± 2.5	65 ± 3.7	75 ± 3.1	61 ± 3.7	63 ± 4.2
Density (kg/m^3)	2367 ± 8	2340 ± 9	2309 ± 10	2251 ± 11	2244 ± 12	2219 ± 10
Strength class [1]	C35/45	C30/37	C20/25	C25/30	C25/30	C12/15
P$_{o,28\,d}$ (vol%) [2]	14.0 ± 0.1	14.8 ± 0.2	15.6 ± 0.4	16.3 ± 0.4	17.4 ± 0.5	18.6 ± 0.4
P$_{o,90\,d}$ (vol%) [3]	13.3 ± 0.2	14.2 ± 0.2	15.0 ± 0.4	14.9 ± 0.3	16.3 ± 0.4	17.5 ± 0.3

Note. [1] Strength class in EC-2 is designated CX/Y, where X is the characteristic 28 day compressive strength value in 15×30 cm cylindrical specimens and Y the characteristic compressive strength in 15×15 cm cubic specimens. [2,3] Po, 28 d/90 d: 28 d/90 d open porosity (porosity accessible to water).

3. Results and Discussion

3.1. Oxygen Permeability

The graphs in Figure 3 of the 28 d and 90 d O$_2$ permeability coefficient and standard deviation (error bars) values denote a decline in permeability with curing age, irrespective of the GRC and MRA content. At the same time, the incorporation of the new recycled components induced a rise in O$_2$ permeability due to (i) the higher porosity of the new cement matrices, attributable to the dilution due to the presence of non-reactive particles in GRC (see item 2.1.1) and (ii) the greater porosity of MRA than NA, induced by the bound mortar and masonry materials found in the former (Table 2). Those findings were consistent with, and within, the range (1.0×10^{-17} to 8.0×10^{-17}) reported for mixes prepared with 50% RCA [35], with 25% masonry aggregate [36], and mixes with 20% masonry waste (in the form of fired clay brick, gloss- or bisque-fired white stoneware or sanitary ware) used as a cement substitute [8].

The use of GRC raised 28 d O_2 permeability by 47.0% in mix N10/0 and 97.3% in mix N25/0 relative to NAC, and by 25.7% in mix R10/50 and 51.9% in mix R25/50 relative to R0/50. These increases were less steep at 90 d: 7.5% in mix N10/0 and 84.1% in mix N25/0 relative to NAC, and 14.9% in mix R10/50 and 47.8% in mix R25/50 relative to R0/50.

Analogously, the use of 50% MRA (mix R0/50) raised 28 d O_2 permeability by 92.7% and the 90 d value by 67.5% relative to the conventional mix with NA. That rise was primarily associated with the effect of the presence of bound mortar and masonry material in MRA (more porous than NA) on O_2 permeability and the more readily accessible ingress pathways generated by microcracks in the MRA microstructure [37,38]. In addition, all the increases lay within the range (18% to 98%) observed in mixes with up to 50% RCA [35,39], with 25% masonry material [36], or prepared with both 25% masonry waste as an OPC replacement and 25% to 50% MRA [9].
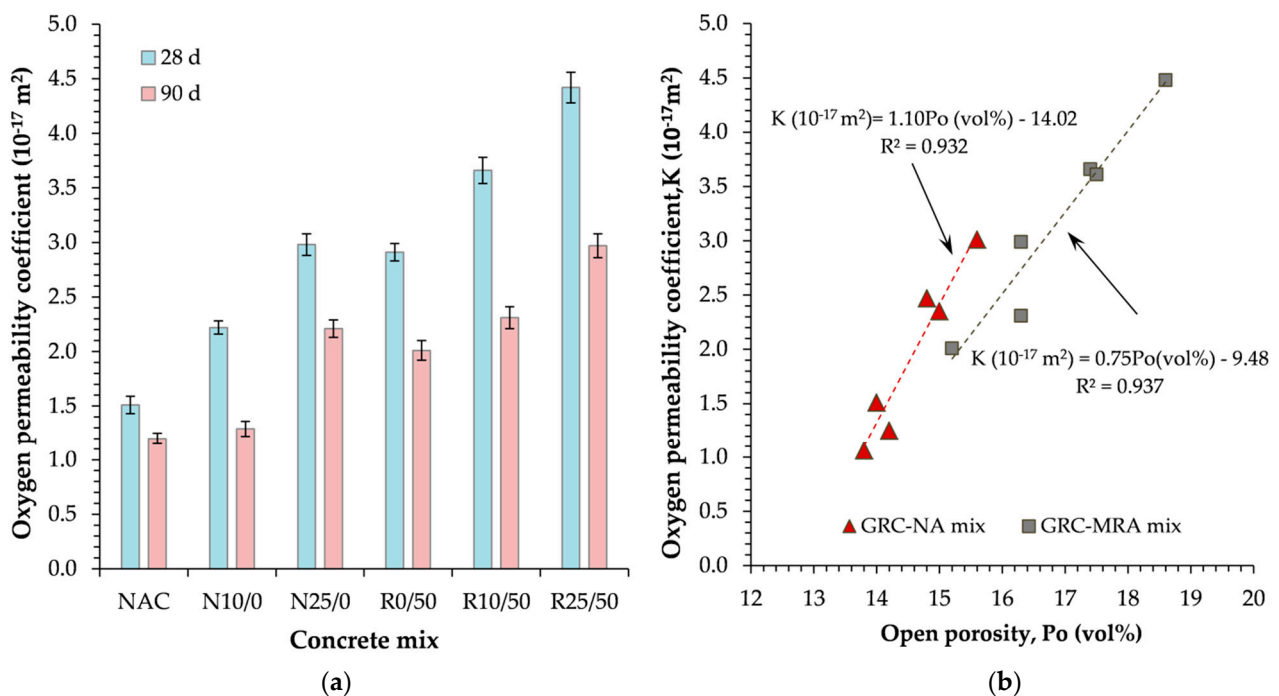

Figure 3. (**a**) 28 d and 90 d oxygen permeability (error bars indicate the standard deviation associated with variability in results); and (**b**) variation in open porosity with oxygen permeability.

Further to the plots in Figure 3b, the O_2 permeability coefficient and open porosity were linearly and closely ($R^2 > 0.91$) correlated in the mixes studied and the former was observed to increase proportionally to the latter. Similar findings were reported for mixes prepared with other additions (fly ash [40], rice husk ash [41] and masonry dust [42]) to replace cement; mixes containing RCA fines and coarse aggregates [43]; and mixes made with masonry aggregate [36]. The inference drawn from such a close correlation indicates that this property may serve as an index for assessing the material's porosity and, consequently, its durability.

3.2. Resistence to Chloride Ion Penetration

The results of the rapid chloride penetration (RCP) test, Berke and Hicks [28] equation-calculated chloride diffusion (D) and the respective standard deviations for the 28 d and 90 d mixes are given in Table 5. The data show a steeper decline in Cl^- penetration with curing age ($\Delta RCP_{28d \rightarrow 90d}$) in the mixes containing recycled materials (GRC and/or MRA) than in the OPC/NA concrete. Similarly, the absolute value of $\Delta RCP_{28d \rightarrow 90d}$ was greater in both the GRC–NA (−13.7% in N10/0 and −14.3% in N25/0) and GRC–MRA (−14.9% in R10/50 and −16.5% in R25/50) families than the −9.3% in the reference NAC.

Table 5. Rapid chloride penetration (RCP) and chloride diffusion in 28 d and 90 d mixes (±, standard deviation).

Concrete Mix	28 d		90 d		$\Delta RCP_{28d \to 90d}$
	RCP (C) *	D (10^{-12} m²/s)	RCP (C)	D (10^{-12} m²/s)	
NAC	3480 ± 258	9.72 ± 0.72	3157 ± 152	8.96 ± 0.84	−9.29
N10/0	3950 ± 245	10.81 ± 0.94	3410 ± 301	9.56 ± 0.91	−13.67
N25/0	4806 ± 453	12.75 ± 1.01	4100 ± 266	11.2 ± 0.98	−14.27
R0/50	4336 ± 361	11.7 ± 0.95	3620 ± 322	10.05 ± 0.81	−16.52
R10/50	4454 ± 284	11.96 ± 1.04	3753 ± 274	10.36 ± 0.92	−15.75
R25/50	4950 ± 181	13.07 ± 0.87	4210 ± 321	11.98 ± 0.82	−14.94

Note. * C: Coulomb.

According to Figure 4a, Cl⁻ penetration rose linearly ($R^2 \geq 0.949$) with the GRC replacement ratio, irrespective of curing age (28 d or 90 d) and family (GRC-NA or GRC-MRA), with values 8.0% higher in mix N10/0 and 38.1% in N25/10 than in NAC, and 2.7% higher in R10/50 and 16.3% in R25/50 than in R0/50. The incorporation of 50% MRA (mix R0/50) also induced increases of 14.7% to 24.6%, relative to mix NAC. That behaviour can be directly associated with the higher porosity of the new cementitious matrices, given the presence of new recycled materials (GRC and/or MRA). It is also consistent with earlier observations for mixes with additions, such as 10% to 40% cement powder [44], 10% to 50% concrete powder [10], or 5% to 15% cement kiln dust [45] as OPC replacements, and materials containing 15% to 30% biomass bottom ash (BBA) to replace OPC, separately or in combination with 30% MRA as an NA substitute [46].
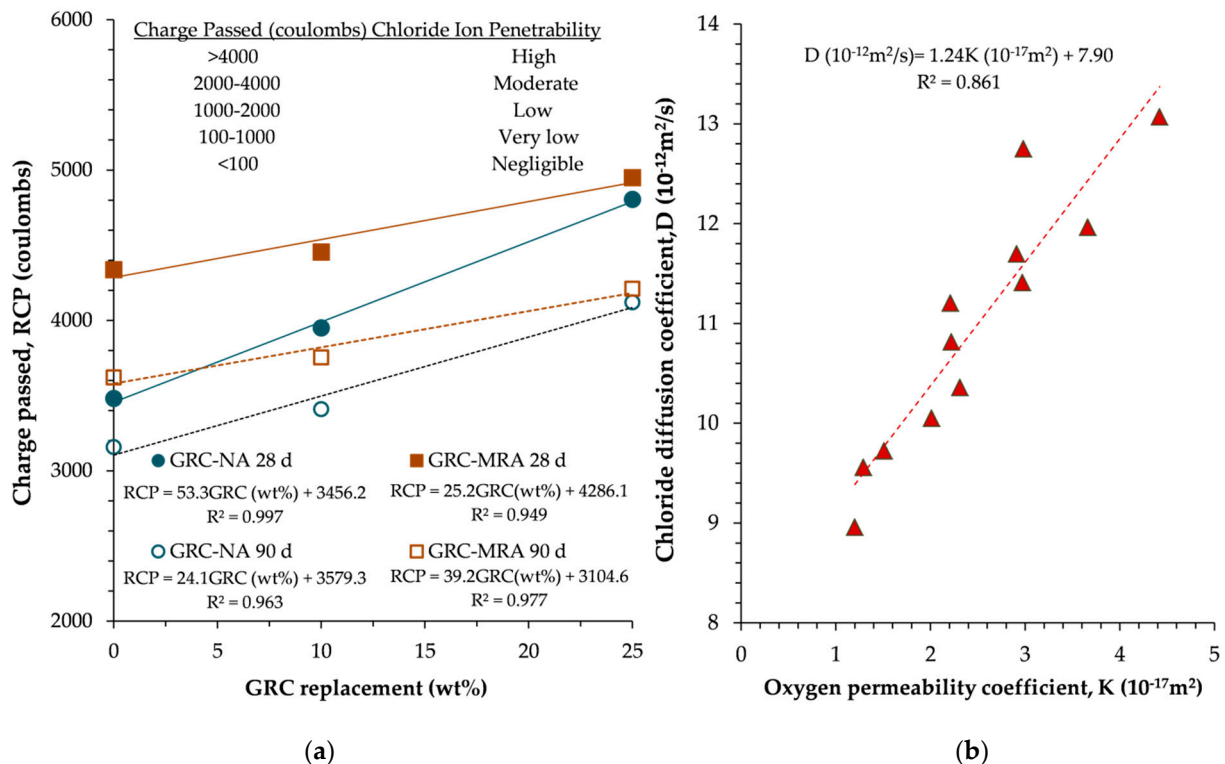

Figure 4. (**a**) Variation in RCP with the inclusion of GRC in 28 d and 90 d mixes; and (**b**) relationship between the chloride diffusion and oxygen permeability coefficients.

The 90 d mixes with 10% GRC, separately or in combination with 50% MRA, qualified for the same 'moderate' corrosion risk class as mix NAC, given that all the rises were observed to lie within the 8% to 30% observed in earlier studies in mixes with 10% to 40% of other inert additions (marble powder and granite dust) [47].

The close linear relationship (R^2 = 0.861 > 0.85 [48,49]) between O_2 permeability and the chloride diffusion coefficient in the mixes studied (Figure 4b) is clear proof that both transport mechanisms depend on pore structure and pore interconnectivity alike [50]. Similar findings were reported earlier for mixes made with additions such as marble powder or granite dust [47], ground granulated blast furnace slag (GGBFS) [51,52] or BBA [46] as cement replacements, mixes with 20% to 100% RCA [43], and mixes where 5% to 10% of the OPC was replaced with silica fume and 50% to 100% of NA with RCA [39].

3.3. Carbonation Resistance

The mean carbonation depths (Cd) of all the mixes after 7 d, 28 d, 56 d or 90 d in an accelerated carbonation chamber and associated standard deviations are listed in Table 6. Carbonation resistance was intensely affected by the porous microstructure of the new recycled concrete mixes with GRC and/or MRA. The use of GRC raised 28 d Cd by +0.8 mm in mix N10/0 and 5.7 mm in mix N25/0 relative to NAC and by 1.0 mm in mix R10/50 and 3.0 mm in mix R25/50 relative to R0/50. Similar findings were observed in mixes prepared with additions such as 5% to 25% marble slurry [53], 25% masonry CDW [12], and 25% to 50% fly ash from biomass-fired power plants [54]. The data in Table 7, in turn, denote the very close (correlation coefficients, R^2, of over 0.89) linear relationship between the Cd and GRC content, irrespective of exposure time and family (GRC-NA or GRC-MRA).

Table 6. Carbonation depth and coefficients in concrete mixes with 7 d, 28 d, 56 d or 90 d exposure to accelerated carbonation ($\pm$, standard deviation).

Concrete Mix	Carbonation Depth (mm)				Carbonation Coefficient	
	7 d	28 d	56 d	90 d	K_{ac} (mm/year$^{0.5}$)	R^2
NAC	2.2 $\pm$ 0.4	5.4 $\pm$ 0.8	6.5 $\pm$ 1.1	9.2 $\pm$ 1.8	17.95	0.988
N10/0	3.1 $\pm$ 0.5	6.2 $\pm$ 0.4	7.2 $\pm$ 1.4	9.9 $\pm$ 1.7	20.55	0.993
N25/0	4.9 $\pm$ 0.3	11.1 $\pm$ 0.4	14.8 $\pm$ 1.7	17.8 $\pm$ 2.1	30.0.8	0.994
R0/50	3.9 $\pm$ 0.2	8.4 $\pm$ 0.8	10.5 $\pm$ 1.4	13.5 $\pm$ 1.5	27.67	0.987
R10/50	4.1 $\pm$ 0.6	9.4 $\pm$ 1.1	10.9 $\pm$ 1.2	14.9 $\pm$ 1.6	29.67	0.994
R25/50	5.1 $\pm$ 0.9	11.4 $\pm$ 0.5	16.6 $\pm$ 1.7	18.0 $\pm$ 2.1	38.96	0.982

Table 7. Correlation between mean carbonation depth and GRC replacement ratio.

Exposure Time (Days)	Type of Mix					
	GRC-NA			GRC-MRA		
	m	a	R^2	m	a	R^2
7	0.11	2.13	0.994	0.04	3.79	0.938
28	0.24	4.81	0.924	0.12	8.32	0.994
56	0.34	5.78	0.944	0.25	9.69	0.882
90	0.35	8.11	0.892	0.18	13.34	0.990

Note. Cd= mx + a, where Cd is mean carbonation depth; m, slope on the regression line; x, GRC replacement ratio; R^2, correlation coefficient.

The incorporation of 50% MRA (R0/50), in turn, induced an increase in Cd of 3.0 mm in the 28 d results, relative to the NAC mix. Such deeper carbonation penetration was associated with higher water absorption and porosity in MRA than in NA [6,49]. This was the same pattern as observed in O_2 penetration discussed in Section 3.1, depicted in Figure 3b and observed by other authors [55,56] in mixes with RA.

The linear relationship in the 28 d and 90 d results between carbonation depth and oxygen permeability is depicted in Figure 5a, and between Cd and the chloride diffusion coefficient in Figure 5b. The high R^2 values (all lying between 0.895 and 0.965) denoted a close correlation between those properties and showed that both the O_2 permeability coefficient and the Cl^- diffusion coefficient may serve to predict the carbonation depth [57,58].

Earlier studies with mixes with additions such as fly ash, GGBFS [40,41] or BBA [46] as cement replacements [51,52] together with 25% to 100% RCA [59] yielded similar findings.
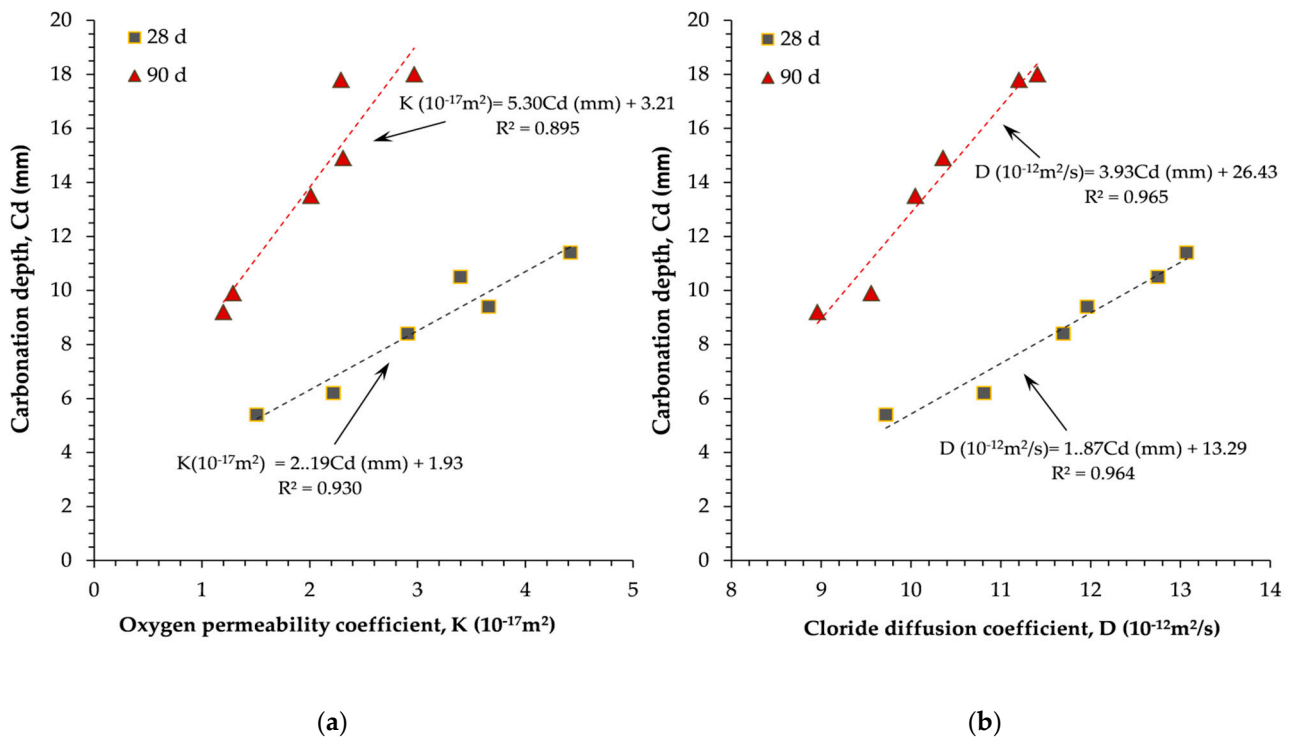

(**a**)

(**b**)

Figure 5. Relationship in 28 d and 90 d mixes between (**a**) carbonation and oxygen permeability coefficient; and (**b**) carbonation and chloride diffusion coefficient.

The accelerated carbonation coefficients (K_{ac}) given in Table 6 were calculated from linear regression of the carbonation depth/square root of time curve and Fick's first law (Equation (7)):

$$C_d = d_0 + K_{ac}\sqrt{t} \tag{7}$$

where Cd is the mean carbonation depth at time t (mm); K_{ac}, the carbonation rate under the experimental conditions (mm/year$^{0.5}$); d_0, the carbonation depth at time = 0 (mm); and t, the exposure time (years).

The reliability of the carbonation coefficients calculated was over 98% in all mixes (see R^2 in Table 6). K_{ac} was 14.5% higher in mix N10/0, 106.6% in N25/0, 54.1% in R0/50, 66.9% in R10/50 and 117.0% in R25/50 than in mix NAC. Those findings denoted a higher rate of carbonation spread in recycled concrete mixes with GRC and/or MRA than in the conventional material. A similar behaviour was reported for mixes with 25% to 50% MRA in combination with 25% fired clay powder processed from CDW and used as a cement substitute [12], and for mixes containing from 50% to 100% RCA, as well as 25% to 55% fly ash [60].

Table 8 lists the carbonation coefficients found for real or natural conditions (K_n) with Equation (8), proposed by Sisomphon and Franke [61] to express the relationship between accelerated and natural carbonation in terms of CO_2 concentration:

$$\frac{K_n}{\sqrt{c_n}} = \frac{K_{ac}}{\sqrt{c_{ac}}} \tag{8}$$

where K_n is the natural carbonation coefficient; K_{ac} the accelerated carbonation coefficient; c_n the CO_2 concentration under natural conditions (~0.04%) [62]; and c_{ac} the CO_2 concentration in the accelerated carbonation test (3%).

Table 8. Natural carbonation coefficients and carbonation resistance classes.

Natural Carbonation Coefficient, K_n (mm/year$^{0.5}$)					
NAC	N10/0	N25/0	R0/50	R10/50	R25/50
2.07	2.37	4.28	3.20	3.46	4.50
Carbonation Resistance Class					
RC2	RC3	RC4	RC5	RC6	RC7
$1 < Kn \leq 2$	$2 < Kn \leq 3$ NAC, N10/0	$3 < Kn \leq 4$ R0/50, R10/50	$4 < Kn \leq 5$ N25/0, R25/50	$5 < Kn \leq 6$	$6 < Kn \leq 7$

All the mixes studied exhibited values lower than or similar to the 4 mm/year$^{0.5}$ indicative of quality concrete [63] and none exceeded the critical value (6 mm/year$^{0.5}$), defined to mixes with low carbonation resistance [59]. Further to the classification proposed by Greve-Dierfeld and Gehlen [64], N10/0 would lie within the same carbonation resistance range (RC3) as NAC, whilst mixes R0/50 and R10/50 would be in class RC4, and mixes N25/0 and R25/50 in class RC5.

3.4. Service Life Prediction

Carbonation spread across concrete exposed to different environments is plotted against exposure time in Figure 6, in keeping with the model set out in Spanish structural concrete code EHE-08 [16]. The dashed horizontal lines show the minimum rated cover for each exposure environment, cement type and design service life. The code defines rated cover as the distance between the outer surface of the reinforcement and the closest concrete surface. In light of the resulting curves, mixes in which 10% GRC or 50% MRA were included separately as well as jointly (R10/50) would be at no risk whatsoever of carbonation-induced reinforcement depassivation in structures with a service life of up to 100 years and design the characteristic strength as listed in Table 4. Mixes with 25% GRC, with or without recycled aggregate, would not be apt for reinforced concrete exposed to carbonation.
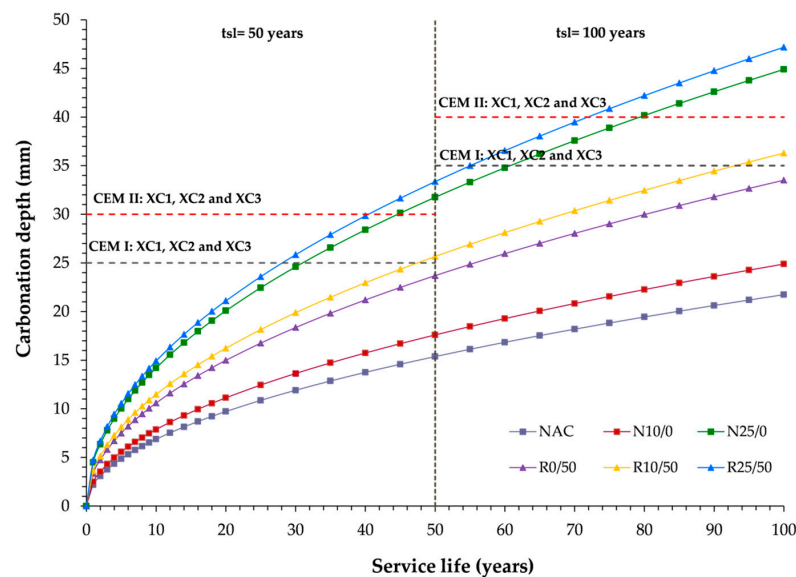

Figure 6. Service life model proposed in Spanish concrete code EHE-08 for carbonation spread in concrete mixes.

4. Conclusions

The conclusions that may be drawn from this study are set out below:

- Incorporating GRC and/or MRA induces an increase in O_2 permeability associated with the greater porosity of these new materials than that found in their conventional counterparts, OPC and NA. Nonetheless, all the O_2 permeability coefficients were below the 4.5×10^{-17} m^2 ceiling for quality concrete;
- Cl$^-$ permeability was not significantly affected (<8%) by the replacement of 10% OPC with GRC, irrespective of the aggregate type present (NA or MRA). The resulting 90 d mixes exhibited the same 'moderate' risk of corrosion as conventional concrete of the same age;
- The high linear correlation between the O_2 permeability and Cl$^-$ diffusion coefficients, irrespective of cement and aggregate type, can be interpreted as proof that these transport mechanisms are governed by both pore structure and interconnectivity;
- The mean carbonation depth in mixes with 10% GRC, separately or jointly with 50% MRA, was 15% to 75% greater than that in mixes prepared with conventional cement and natural aggregate;
- All mixes, irrespective of the GRC replacement ratio and aggregate type, exhibited CO_2 penetration coefficients lower than or similar to 4 mm/year$^{0.5}$;
- The high correlation between O_2 permeability and carbonation depth suggests that the former may be a good indicator for predicting the latter;
- According to the service life prediction model proposed in Spanish structural concrete code EHE-08, incorporating up to 10% GRC as a cement replacement and/or 50% MRA as an NA substitute does not compromise the reinforcement's passivity.

Author Contributions: B.C. performed the experiments; M.B. and B.C. analysed the data and wrote the paper; I.F.S.d.B., C.M. and J.d.B. supervised the research work and revised the paper. All the authors contributed to the experiment design and analysed and discussed the findings. All authors have read and agreed to the published version of the manuscript.

Institutional Review Board Statement: Not applicable.

Informed Consent Statement: Not applicable.

Data Availability Statement: Data sharing not applicable.

Conflicts of Interest: The authors have no conflict of interest that may have influenced the research described in this paper.

References

1. Real, S.; Gomes, M.G.; Moret Rodrigues, A.; Bogas, J.A. Contribution of Structural Lightweight Aggregate Concrete to the Reduction of Thermal Bridging Effect in Buildings. *Constr. Build. Mater.* **2016**, *121*, 460–470. [CrossRef]
2. Kropp, J. Relations between Transport Characteristics and Durability. *Perform. Criteria Concr. Durab. RILEM Rep.* **1995**, *12*, 97–137.
3. Mehta, P.K.; Monteiro, P.J. *Concrete Microstructure, Properties and Materials*; McGraw-Hill Education: New York, NY, USA, 2017.
4. Bogas, J.A.; Real, S. A Review on the Carbonation and Chloride Penetration Resistance of Structural Lightweight Aggregate Concrete. *Materials* **2019**, *12*, 3456. [CrossRef]
5. UN-DESA-PD. *World Urbanization Prospects: The 2015 Revision, Highlights. Working Paper ESA/P/WP*; UN DESA's Population Division: New York, NY, USA, 2015; p. 66.
6. Bravo, M.; de Brito, J.; Pontes, J.; Evangelista, L. Durability Performance of Concrete with Recycled Aggregates from Construction and Demolition Waste Plants. *Constr. Build. Mater.* **2015**, *77*, 357–369. [CrossRef]
7. Friedrich, J.; Damassa, T. *The History of Carbon Dioxide Emissions*; World Resources Institute: Washington, DC, USA, 2014.
8. Pacheco-Torgal, F.; Jalali, S. Compressive Strength and Durability Properties of Ceramic Wastes Based Concrete. *Mater. Struct.* **2011**, *44*, 155–167. [CrossRef]
9. Thomas, C.; Cimentada, A.I.; Cantero, B.; Sáez del Bosque, I.F.; Polanco, J.A. Industrial Low-Clinker Precast Elements Using Recycled Aggregates. *Appl. Sci.* **2020**, *10*, 6655. [CrossRef]
10. Qin, L.; Gao, X. Recycling of Waste Autoclaved Aerated Concrete Powder in Portland Cement by Accelerated Carbonation. *Waste Manag.* **2019**, *89*, 254–264. [CrossRef] [PubMed]
11. Kim, Y.-J. Quality Properties of Self-Consolidating Concrete Mixed with Waste Concrete Powder. *Constr. Build. Mater.* **2017**, *135*, 177–185. [CrossRef]
12. Sáez del Bosque, I.F.; Van den Heede, P.; De Belie, N.; Sánchez de Rojas, M.I.; Medina, C. Carbonation of Concrete with Construction and Demolition Waste Based Recycled Aggregates and Cement with Recycled Content. *Constr. Build. Mater.* **2020**, *234*, 117336. [CrossRef]
13. Cantero, B.; Bravo, M.; de Brito, J.; Sáez del Bosque, I.F.; Medina, C. Mechanical Behaviour of Structural Concrete with Ground Recycled Concrete Cement and Mixed Recycled Aggregate. *J. Clean. Prod.* **2020**, *275*, 122913. [CrossRef]
14. Cantero, B.; Bravo, M.; de Brito, J.; Sáez del Bosque, I.F.; Medina, C. Water Transport and Shrinkage in Concrete Made with Ground Recycled Concrete-Additioned Cement and Mixed Recycled Aggregate. *Cem. Concr. Compos.* **2021**, 103957. [CrossRef]
15. Cantero, B.; Bravo, M.; de Brito, J.; Sáez del Bosque, I.F.; Medina, C. Thermal Performance of Concrete with Recycled Concrete Powder as Partial Cement Replacement and Recycled CDW Aggregate. *Appl. Sci.* **2020**, *10*, 4540. [CrossRef]
16. *Comisión Permanente del Hormigón Instrucción Hormigón Estructural. EHE-08 (Spanish Code on Structural Concrete)*; Gobierno de España: Madrid, Spain, 2008.
17. European Committee for Standardization. *EN 933. Tests for Geometrical Properties of Aggregates. Part 1: Determination of Particle Size Distribution—Sieving Method*; European Committee for Standardization: Brussels, Belgium, 2012.
18. European Committee for Standardization. *EN 933. Tests for Geometrical Properties of Aggregates—Part 11: Classification Test for the Constituents of Coarse Recycled Aggregate*; European Committee for Standardization: Brussels, Belgium, 2010.
19. European Committe for Standardization. *EN 12620. Aggregates for Concrete*; European Committee for Standardization: Brussels, Belgium, 2013.
20. European Committee for Standardization. *EN 1097. Tests for Mechanical and Physical Properties of Aggregates. Part 6: Determination of Particle Density and Water Absorption*; European Committee for Standardization: Brussels, Belgium, 2014.
21. Rodrigues, F.; Evangelista, L.; de Brito, J. A New Method to Determine the Density and Water Absorption of Fine Recycled Aggregates. *Mater. Res.* **2013**, *16*, 1045–1051. [CrossRef]
22. European Committee for Standardization. *EN 1097. Tests for Mechanical and Physical Properties of Aggregates. Part 2: Methods for the Determination of Resistance to Fragmentation*; European Committee for Standardization: Brussels, Belgium, 2010.
23. European Committee for Standardization. *EN 933. Tests for Geometrical Properties of Aggregates. Part 3: Determination of Particle Shape—Flakiness Index*; European Committee for Standardization: Brussels, Belgium, 2012.
24. European Committe for Standardization. *EN 12390. Testing Hardened Concrete. Part 2: Making and Curing Specimens for Strength Tests*; European Committee for Standardization: Brussels, Belgium, 2009.
25. Spanish Committee for Standardization. *UNE 83981. Concrete Durability. Test Methods. Determination to Gas Permeability of Hardened Concrete*; Spanish Committee for Standardization: Madrid, Spain, 2008.
26. Kollek, J.J. The Determination of the Permeability of Concrete to Oxygen by the Cembureau Method—A Recommendation. *Mater. Struct.* **1989**, *22*, 225–230. [CrossRef]
27. *ASTM C 1202-97. Standard Test Method for Electrical Indication of Concrete's Ability to Resist Chloride Ion Penetration*; ASTM International: West Conshohocken, PA, USA, 1997.
28. Berke, N.S.; Hicks, M.C. Estimating the life cycle of reinforced concrete decks and marine piles using laboratory diffusion and corrosion data. In *Corrosion Forms and Control for Infrastructure*; ASTM International: West Conshohocken, PA, USA, 1992.
29. National Laboratory in Civil Engineering (LNEC—Laboratório Nacional de Engenharia Civil). *LNEC-E391. Concrete: Determination of Carbonation Resistance (in Portuguese)*; National Laboratory in Civil Engineering (LNEC—Laboratório Nacional de Engenharia Civil): Lisbon, Portugal, 1993.

30. Keßler, S.; Fischer, J.; Straub, D.; Gehlen, C. Updating of Service-Life Prediction of Reinforced Concrete Structures with Potential Mapping. *Cem. Concr. Compos.* **2014**, *47*, 47–52. [CrossRef]
31. Faury, J. *Le Béton. Ed.*; Dunod: París, France, 1958.
32. European Committee for Standardization. *EN 206 Concrete. Part 1: Specification, Performance, Production and Conformity*; European Committee for Standardization: Brussels, Belgium, 2013.
33. European Committee for Standardization. *EN 12350. Testing Fresh Concrete. Part 2: Slump-Test*; European Committee for Standardization: Brussels, Belgium, 2009.
34. Bravo, M.; de Brito, J.; Pontes, J.; Evangelista, L. Mechanical Performance of Concrete Made with Aggregates from Construction and Demolition Waste Recycling Plants. *J. Clean. Prod.* **2015**, *99*, 59–74. [CrossRef]
35. Thomas, C.; Setién, J.; Polanco, J.A.; Alaejos, P.; Sánchez de Juan, M. Durability of Recycled Aggregate Concrete. *Constr. Build. Mater.* **2013**, *40*, 1054–1065. [CrossRef]
36. Medina, C.; Frías, M.; Sánchez de Rojas, M.I.; Thomas, C.; Polanco, J.A. Gas Permeability in Concrete Containing Recycled Ceramic Sanitary Ware Aggregate. *Constr. Build. Mater.* **2012**, *37*, 597–605. [CrossRef]
37. Kapoor, K.; Singh, S.P.; Singh, B. Durability of Self-Compacting Concrete Made with Recycled Concrete Aggregates and Mineral Admixtures. *Constr. Build. Mater.* **2016**, *128*, 67–76. [CrossRef]
38. Kumar Mehta, P.D.; Paulo, J.M.; Monteiro, P.D. Proportioning Concrete Mixtures. In *Concrete: Microstructure, Properties, and Materials*, 4th ed.; McGraw Hill Professional, Access Engineering: New York, NY, USA, 2014.
39. Pedro, D.; de Brito, J.; Evangelista, L. Durability Performance of High-Performance Concrete Made with Recycled Aggregates, Fly Ash and Densified Silica Fume. *Cem. Concr. Compos.* **2018**, *93*, 63–74. [CrossRef]
40. Van den Heede, P.; Gruyaert, E.; De Belie, N. Transport Properties of High-Volume Fly Ash Concrete: Capillary Water Sorption, Water Sorption under Vacuum and Gas Permeability. *Cem. Concr. Compos.* **2010**, *32*, 749–756. [CrossRef]
41. Jaya, R.; Bakar, B.; Johari, M.; Ibrahim, M. Strength and Permeability Properties of Concrete Containing Rice Husk Ash with Different Grinding Time. *Open Eng.* **2011**, *1*, 103–112. [CrossRef]
42. Li, L.; Liu, W.; You, Q.; Chen, M.; Zeng, Q.; Zhou, C.; Zhang, M. Relationships between Microstructure and Transport Properties in Mortar Containing Recycled Ceramic Powder. *J. Clean. Prod.* **2020**, *263*, 121384. [CrossRef]
43. Berredjem, L.; Arabi, N.; Molez, L. Mechanical and Durability Properties of Concrete Based on Recycled Coarse and Fine Aggregates Produced from Demolished Concrete. *Constr. Build. Mater.* **2020**, *246*, 118421. [CrossRef]
44. Siddique, R.; Nanda, V.; Kunal; Kadri, E.H.; Khan, M.I.; Singh, M.; Rajor, A. Influence of Bacteria on Compressive Strength and Permeation Properties of Concrete Made with Cement Baghouse Filter Dust. *Constr. Build. Mater.* **2016**, *106*, 461–469. [CrossRef]
45. Maslehuddin, M.; Al-Amoudi, O.S.B.; Rahman, M.K.; Ali, M.R.; Barry, M.S. Properties of Cement Kiln Dust Concrete. *Constr. Build. Mater.* **2009**, *23*, 2357–2361. [CrossRef]
46. Agrela, F.; Beltran, M.G.; Cabrera, M.; López, M.; Rosales, J.; Ayuso, J. Properties of Recycled Concrete Manufacturing with All-in Recycled Aggregates and Processed Biomass Bottom Ash. *Waste Biomass Valorization* **2018**, *9*, 1247–1259. [CrossRef]
47. Rashwan, M.A.; Al Basiony, T.M.; Mashaly, A.O.; Khalil, M.M. Behaviour of Fresh and Hardened Concrete Incorporating Marble and Granite Sludge as Cement Replacement. *J. Build. Eng.* **2020**, *32*, 101697. [CrossRef]
48. Montgomery, D.C.; Peck, E.A. *Introduction to Linear Regression Analysis*; John Wiley & Sons: New York, NY, USA, 1982.
49. Gomes, M.; de Brito, J. Structural Concrete with Incorporation of Coarse Recycled Concrete and Ceramic Aggregates: Durability Performance. *Mater. Struct.* **2009**, *42*, 663–675. [CrossRef]
50. Meng, D.; Wu, X.; Quan, H.; Zhu, C. A Strength-Based Mix Design Method for Recycled Aggregate Concrete and Consequent Durability Performance. *Constr. Build. Mater.* **2021**, *281*, 122616. [CrossRef]
51. Ibrahim, M.; Issa, M. Evaluation of Chloride and Water Penetration in Concrete with Cement Containing Limestone and IPA. *Constr. Build. Mater.* **2016**, *129*, 278–288. [CrossRef]
52. Jang, S.-Y.; Karthick, S.; Kwon, S.-J. Investigation on Durability Performance in Early Aged High-Performance Concrete Containing GGBFS and FA. Available online: https://www.hindawi.com/journals/amse/2017/3214696/ (accessed on 24 February 2021).
53. Rana, A.; Kalla, P.; Csetenyi, L.J. Sustainable Use of Marble Slurry in Concrete. *J. Clean. Prod.* **2015**, *94*, 304–311. [CrossRef]
54. Teixeira, E.R.; Camões, A.; Branco, F.G.; Aguiar, J.B.; Fangueiro, R. Recycling of Biomass and Coal Fly Ash as Cement Replacement Material and Its Effect on Hydration and Carbonation of Concrete. *Waste Manag.* **2019**, *94*, 39–48. [CrossRef] [PubMed]
55. Shi, H.; Xu, B.; Zhou, X. Influence of Mineral Admixtures on Compressive Strength, Gas Permeability and Carbonation of High Performance Concrete. *Constr. Build. Mater.* **2009**, *23*, 1980–1985. [CrossRef]
56. Kumar, P.; Singh, N. Influence of Recycled Concrete Aggregates and Coal Bottom Ash on Various Properties of High Volume Fly Ash-Self Compacting Concrete. *J. Build. Eng.* **2020**, *32*, 101491. [CrossRef]
57. Belgacem, M.E.; Neves, R.; Talah, A. Service Life Design for Carbonation-Induced Corrosion Based on Air-Permeability Requirements. *Constr. Build. Mater.* **2020**, *261*, 120507. [CrossRef]
58. Nguyen, M.H.; Nakarai, K.; Torrent, R. Service Life Prediction of Steam-Cured Concrete Utilizing in-Situ Air Permeability Measurements. *Cem. Concr. Compos.* **2020**, *114*, 103747. [CrossRef]
59. Jiménez, L.F.; Moreno, E.I. Durability Indicators in High Absorption Recycled Aggregate Concrete. *Adv. Mater. Sci. Eng.* **2015**, *2015*, e505423. [CrossRef]
60. Kou, S.-C.; Poon, C.-S. Long-Term Mechanical and Durability Properties of Recycled Aggregate Concrete Prepared with the Incorporation of Fly Ash. *Cem. Concr. Compos.* **2013**, *37*, 12–19. [CrossRef]

61. Sisomphon, K.; Franke, L. Carbonation Rates of Concretes Containing High Volume of Pozzolanic Materials. *Cem. Concr. Res.* **2007**, *37*, 1647–1653. [CrossRef]
62. Zhang, K.; Xiao, J. Prediction Model of Carbonation Depth for Recycled Aggregate Concrete. *Cem. Concr. Compos.* **2018**, *88*, 86–99. [CrossRef]
63. Neville, A.M. *Properties of Concrete*, 5th ed.; Pearson: London, UK, 1995; ISBN 978-0-273-75580-7.
64. von Greve-Dierfeld, S.; Gehlen, C. Performance-Based Durability Design, Carbonation Part 2—Classification of Concrete. *Struct. Concr.* **2016**, *17*, 523–532. [CrossRef]